Journal of Engg. Research **Vol. 5 No. (3) September 2017 pp.** *216-229*

دراسة تأثير نسبة جدار جانب الشق على استقرار التدفق ونقل الحرارة في الاسطوانات الدائرة متحدة المركز

دونغ ليو*،*، جيان تشو*، يينغ زي وانغ*، تشانغ تشينغ تشاو* وشياو بينغ جيانغ****

* كلية الطاقة وهندسة الطاقة، جامعة جيانغسو، تشنجيانغ، 212013، الصين

** مركز البحوث الوطنية للمضخات، جامعة جيانغسو، تشنجيانغ، 212013، الصين

*** مراسلة المؤلف على البريد الالكتروني: *liudong@ujs.edu.cn*

الخـلاصـة

تم دراسة تأثير نسبة جدار جانب الشق على عدم استقرار التدفق وخصائص نقل الحرارة من تدفق (تايلور-كويت) بواسطة طريقة المحاكاة العددية. تم تأكيد دقة نتيجة المحاكاة العددية بواسطة تجربة (PIV). تم دراسة أربعة نماذج مختلفة بنسب جانبية قدرها 0.5، 0.75، 1، 1.25 على التوالي. وجد أن المقاس المحوري لدوامة تايلور (Taylor) لا تتغير مع تغير نسبة جدار جانب الشق في حالة تساوي الحرارة، ولكن تزداد مع نسبة جدار جانب الشق في حالة غير تساوي الحرارة. ولنسبة جانب الشق الجانب أيضا تأثير كبير على توزيع السرعة الدائرية في الفجوة الحلقية. أقصى سرعة دائرية كانت في النموذج ذو نسبة جدار 0.75 أكبر من النماذج الأخرى. وبالمقارنة مع توزيع درجة الحرارة في النماذج المختلفة، وجد أن التدرج الحراري للسائل بالقرب من الجدار الداخلي الاسطوانة يكون أقصى قيمة في النموذج ذو نسبة 0.75. متوسط رقم (Nusselt) أيضا يكون أكبر قيمة في نفس النموذج. وكلما زادت النسبة من 0.5 إلى 0.75، يتم تعزيز قدرة نقل الحرارة من السائل بشكل واضح. وكلما تزداد نسبة الجدار أكثر، فإن قدرة نقل الحرارة من السائل يضعف قليلا.

Study of slit wall aspect ratio effect on the flow stability and heat transfer in rotating concentric cylinders

Dong Liu*,***, Jian Zhu*, Ying-ze Wang*, Chang-qing Chao* and Xiao-Ping Jiang**

**School of Energy and Power Engineering, Jiangsu University, Zhenjiang, 212013, China*

***National Research Center of Pumps, Jiangsu University, Zhenjiang, 212013, China*

****Corresponding author: liudong@ujs.edu.cn*

ABSTRACT

The slit wall aspect ratio effect on the flow instability and heat transfer characteristics of Taylor-Couette flow was studied by numerical simulation method. The accuracy of the numerical simulation result was confirmed by PIV experiment. Four different models with aspect ratios of 0.5, 0.75, 1 and 1.25, respectively were investigated. It is found that the axial size of Taylor vortex does not vary with the slit aspect ratio at isothermal condition, but increased with slit wall aspect ratio at non-isothermal condition. The slit aspect ratio also has significant influence on the distribution of radial velocity in the annular gap. The maximum radial velocity in the model with aspect ratio of 0.75 is larger than other models. Comparing with the temperature distribution in different models, the temperature gradient of the fluid near the inner cylinder to the wall has the maximum value in the model with aspect ratio of 0.75. The average Nusselt number also has the largest value in the same model. As the aspect ratio increases from 0.5 to 0.75, the heat transfer ability of the fluid is enhanced obviously. As the aspect ratio increases further, the heat transfer ability of the fluid is weaken slightly.

NOMENCLATURE

C_p	Specific heat capacity
d	Annular gap width
Gr	Grashof number
h^*	Ratio of slit depth to width
L	Length of the cylinder
Nu	Local Nusselt number
$\overline{Nu}$	Average Nusselt number
p	Slit depth
Pr	Prandtl number

r_i	Radius of inner cylinder
r_o	Radius of outer cylinder
Re	Rotational Reynolds number
R^*	Dimensionless radial position
T_{in}	Temperature of inner cylinder wall
T_{out}	Temperature of outer cylinder wall
T_{w}	Temperature of liquid
v	Kinematic viscosity
V_r	Radial velocity
V_z	Axial velocity
w	Slit width
Z^*	Dimensionless axial position
α	Thermal diffusivity
β	Coefficient of thermal expansion
λ	Axial dimension of Taylor vortex
μ	Dynamic viscosity
ρ	Fluid density
τ	Dimensionless radial temperature
ω	Vorticity
Ω	Angular velocity of the inner cylinder
ΔT	Temperature gradient

INTRODUCTION

Taylor–Couette flow is one of the classic problems in fluid mechanics (Taylor, 1923). Because this kind flow widely occurs in lots of mechanical devices such as electric motor, rotating blade couplers, and bearings, the study on heat transfer process of Taylor-Couette flow has an important effect on the improvement of the mechanical performance and operation stability. Many scholars and researchers have carried out lots of theoretical analysis, numerical calculation, and experimental research.

Deters *et al*. (2005) investigated the interaction between the temperature field and the velocity field to understand the influence of thermal convection, which made the fluid near the inner cylinder wall flow upward and the fluid near the outer cylinder wall flow downward. Kádár & Balan (2012) found Taylor vortex flow in the vicinity of critical Reynolds number after the transitions from Taylor vortex flow to wavy vortex flow. Tzeng (2006) calculated the heat transfer coefficient of

internal and external cylindrical surface using experimental data, and the results showed that the heat transfer coefficient increased with increasing the rotational Reynolds number. Kiełczewski *et al*. (2014) used numerical simulation to study the flow field structure and flow characteristics by changing the parameters, which included aspect ratio, side wall boundary conditions, and temperature gradient. All of the aforementioned scholars revealed the characteristics of the Taylor-Couette flow in the annular gap and the heat transfer process in plain wall models. In engineering applications, in order to enhance the heat transfer process in the annular gap, the structure of the outer wall is complex. In view of this fact, scholars have considered the impact of wall structure on the Taylor-Couette flow and the heat transfer process.

Lee *et al*. (1989) studied the influence of the slit wall on the Taylor-Couette flow under the condition of heat transfer, and they found that the heat transfer was enhanced by the slit surface. Fenot *et al*. (2013) studied the thermal convection with different wall structures and concluded that the heat transfer intensity was a function of axial and rotational velocities. Sun *et al*. (2012) analyzed the reason for the enhancement of heat transfer between the concentric cylinder annular gaps by using numerical simulation. The characteristics of the Taylor-Couette flow and heat transfer in concentric cylinders were also studied by Jeng (2007) who found that the *Nu* number was minimum at the annular entrance along the axis. Liu *et al*. (2015) studied the slit wall effect on Taylor vortex flow and found that the Taylor vortex moved along the axial direction.

The above-listed studies show that many scholars focused on studying the effects of outer wall structure on the heat transfer process in the annular gap. Some of these investigations were about the mechanism of slit number effect on the flow transition process. However, only few of the above-listed studies mentioned the slit aspect ratio effect on the heat transfer process. In this paper, slit wall aspect ratio effect on the Taylor-Couette flow and heat transfer process was studied by numerical simulation.

The present paper is organized as follows. First, the model parameters and the numerical method are briefly described. The accuracy of the numerical simulation method is verified by the PIV measurement result. This is followed by the results' discussion of different slit models. Finally, the conclusion is reported.

NUMERICAL SIMULATION METHODOLOGY

The numerical model

The schematic diagrams of slit model are shown in Figure 1. The inner cylinder has a radius of r_i =33mm and the outer cylinder has a radius of r_o=40mm. Hence, the gap between the two cylinders is d =7mm. The length of the cylinder is L=336mm. The slit number is 6, the width of each slit is 5mm (w=5mm), the depth of each slit is also 5mm (p=5mm), and four models with different slit depths are selected to study the slit depth effect on the Taylor-Couette flow. The dimensionless h^* is the slit wall aspect ratio, defined as $h^*=p/w$, and h^* is 0.5, 0.75, 1.0, and 1.25 in this study.

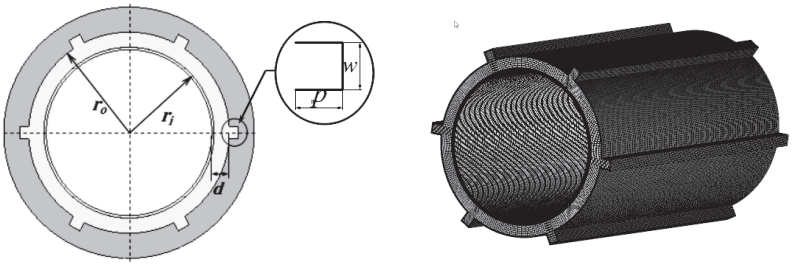

(a) (b)

Figure 1. Schematic diagram of the slit model with relevant parameters.

The numerical method

In numerical simulation, the mesh density affects the computation time and accuracy. Normally, a higher mesh density results in higher computation accuracy. However, a higher mesh density also means longer computing time, and higher demands on computer hardware. Hence, reasonable meshing is the key to get accurate calculation results.

The structure mesh is applied in this study, which is shown in Figure 1(b). The numerical simulation of a different grid density was carried out under the same working conditions; the feasibility and accuracy of the selected grid density were verified by comparing the experimental and numerical results. According to our previous study (Liu *et al*., 2015), the grid number adopted in the present investigation was a structured mesh with 250 × 30 × 330 grid points (along the azimuthal, radial, and axial directions). For model $h^* = 1.0$, the mesh in slit wall region was 10 × 10 × 330 × 6 grid points (along the azimuthal, radial, and axial directions and slit number). The total mesh number is 2,673,000, which conforms to the requirements of the calculations.

The working fluid is sodium iodide solution, with a density of 1780 kg/m^3, dynamic viscosity of 0.00271Pa·s, thermal conductivity of 0.209 w/(m·K), specific heat capacity of 2725J/(kg·K), and thermal expansion coefficient of 0.00057 (1/K). The outer cylinder with a temperature (T_{out}) of 24^{o}C is resting, and the inner cylinder with a surface temperature (T_{in}) of 25.2^{o}C is rotating. A stationary wall with an adiabatic condition is adapted to the ends of the model. The Grashof number, defined as $Gr=(d^3\beta g\Delta T)/\nu^2$, was used to describe the effect of temperature gradient, where g is the acceleration of gravity and ΔT is the temperature difference between the two cylinders; in this paper, ΔT is 1.2°C, so the Grashof number is 1000. The Prandtl number, defined as $Pr=\nu/\alpha=(\mu C_p)/k$, was used to reflect the effect of physical properties on the convective heat transfer of the fluid, where C_p is the specific heat capacity, and the Prandtl number is taken as 35.6 in the present study. Finally, the Reynolds number is defined as $Re= (r_i d\Omega)/\nu$. In the present work, the minimum and maximum values of the Reynolds number are 115 and 574, respectively. The foregoing values of the Reynolds number correspond to the angular velocity of the inner cylinder between 0.7567 rad/s and 3.777 rad/s, respectively.

The laminar model was applied to the simulation in the Taylor vortex since the flow in the annular gap is laminar, and the energy equation is turned on. The Boussinesq assumption was applied to consider the natural convection effect. Under-relaxation factors are 0.3 for pressure,

0.7 for momentum, and 0.9 for energy. The way of discretization is second-order for pressure, SIMPLEC for pressure-velocity coupling, second-order upwind for momentum, and second-order upwind for energy. The characteristics of the Taylor vortex flow are described by the convergent calculation results.

NUMERICAL VALIDITY

In the present study, steady-state flow calculations under isothermal conditions and unsteady-state flow calculations under non-isothermal conditions are considered. The former study obtained the depth of slit wall effect on the characteristics of vortex flow in the annular gap, and the latter obtained the depth of slit wall effect on the heat transfer process. Compared with the experimental results, the numerical simulation result is verified.

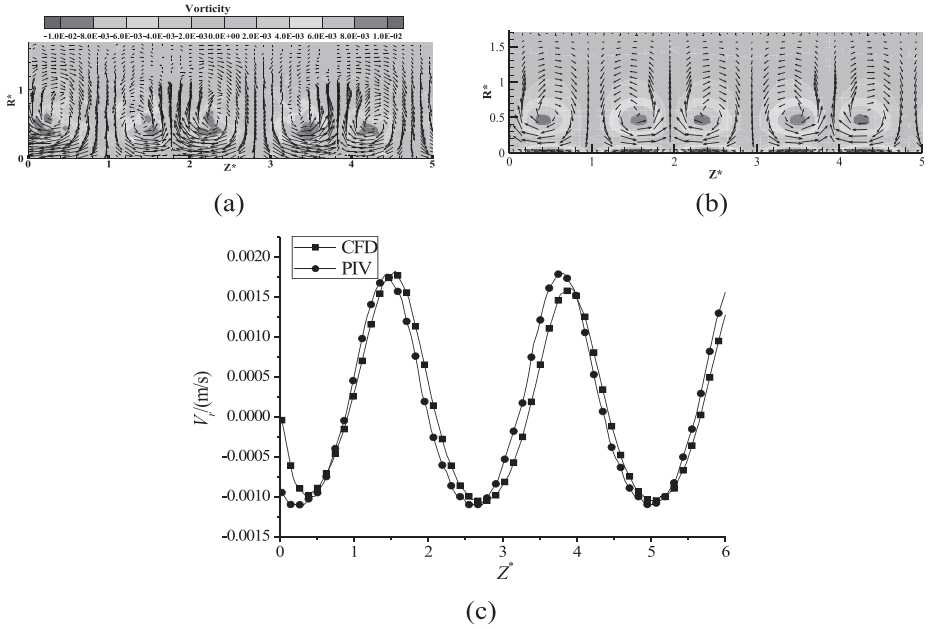

Figure 2. The velocity field in radial-axial plane of the model h^*=1.
(a) Experimental result, (b) CFD result, (c) radial velocity distribution at Re=115.

Figure 2 shows the velocity fields of the Taylor vortex flow in the model h^*=1 when the Reynolds number is 115. The dimensionless coordinate of the axial position is defined as $Z^*=z/d$, and the radial position is $R^*= (r_o-r_i)/d$. The vorticity is expressed as $\omega=dv_r/dz-dv_z/dr$, where V_r is the radial velocity and V_z is the axial velocity. Figure 2(a) was obtained by the PIV experimental measurement, and Figure 2(b) was the result of the numerical simulation. It can be found that the flow fields obtained from the experiment and calculations are consistent. In order to verify the accuracy of the numerical calculations, the radial velocity distribution at location R^*=0.5 was extracted from the numerical simulation and experimental results, which is shown in Figure 2(c). It was found that the difference between radial velocity distributions

obtained by both methods is very small, except when the maximum radial velocity of the experimental data is larger than that of the CFD results. In order to further verify the numerical simulation accuracy, the axial dimension of the Taylor vortex (λ) is calculated. The experimental value of λ_1 is equal to 1.92d, and the numerically calculated value of λ_2 is equal to 1.91d. Hence, the error is 0.5%. Finally, the numerical simulation method is proved to be reasonable and effective for the isothermal conditions.

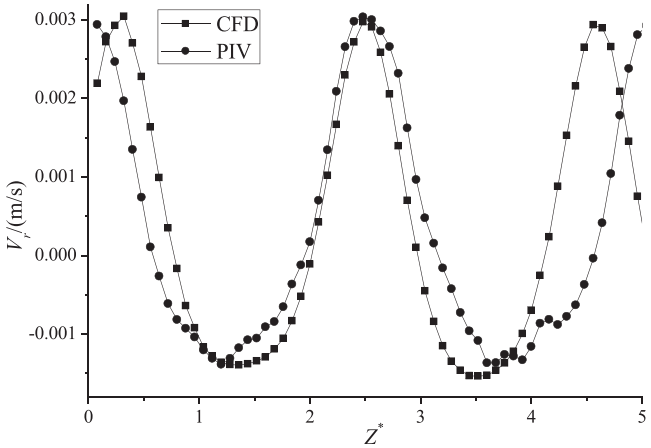

Figure 3. The radial velocity distribution in radial-axial plane of the model h^*=1 (Re=132).

Figure 3 shows a comparison between the velocity field of the experiment and that obtained from the numerical simulation under non-isothermal conditions at Re=132. The experimental value of λ_1 is equal to 1.81d, and the calculated value of λ_2 is equal to 1.71d. The results obtained from those values show a little difference, because when the Reynolds number is 132, the helical wavy vortex flow appears in the model from the experimental results of Liu (2010), which was the unsteady flow. The minimum interval time between each experimental data is 0.2s, and the time step size of CFD is 0.05s. Furthermore, the initial time of CFD and experimental data cannot exactly be the same, and it is difficult to get the CFD and experimental measurement results at the same time. Another reason is that the average temperature near the inner and outer cylinder walls was used in the CFD work, but the real conditions in the experiment are that the temperature distribution cannot be uniform near both cylinder surfaces. The present authors think that the difference between the numerical simulation and the experimental results was within a reasonable range. Therefore, the numerical simulation method used in this paper is reliable for finding the slit aspect ratio effect on the heat transfer process.

ANALYSIS OF SIMULATION RESULTS

Flow field under isothermal conditions

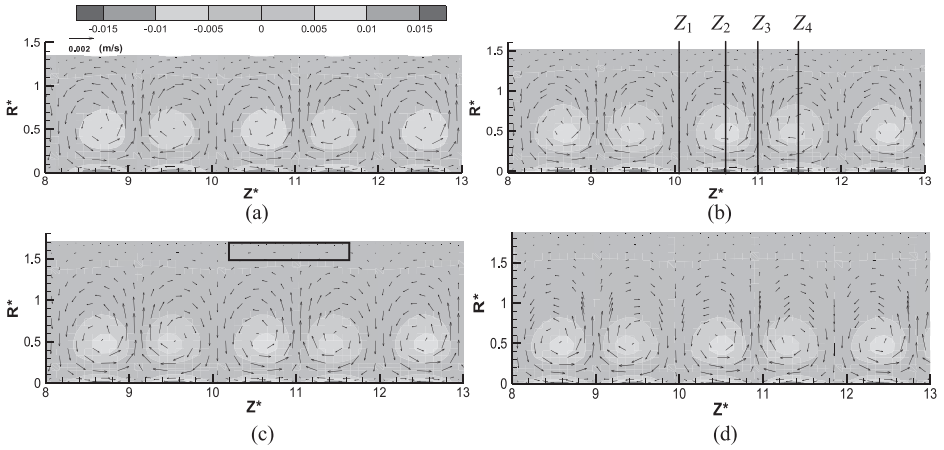

Figure 4. Velocity and vorticity distribution in R-Z plane. (a) h^*=0.5, (b) h^*=0.75, (c) h^*=1.0, (d) h^*=1.25.

Figure 4 shows the velocity and vorticity distribution in the R-Z plane of different slit models. The same axial position is away from the model top by a length of 35mm. The vortex size of each model is basically the same. The maximum vorticity is located at the center position of the vortex cell, and the vortex center is located at the middle position of the annular gap. The Taylor vortex axial dimension of all the models is equal to 1.91*d*, which means that the slit depth has no effect on the size of the Taylor vortex under isothermal conditions.

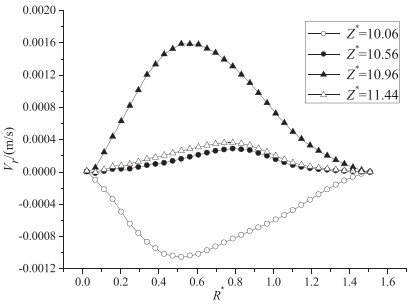

Figure 5. The radial velocity distribution along the radial direction (h^*=0.75).

Figure 5 shows the radial velocity distribution along the radial direction at different axial positions of the model h^*= 0.75, and the positive radial velocity means that the fluid flows from the inner cylinder to the outer one. It can be found that the radial velocity distribution has a parabolic shape. The radial velocity has the largest negative amplitude at Z_1=10.06, where it is located between two vortices in a vortex pair. The radial velocity fluctuation is minimum at Z_2 =10.56 and Z_4=11.44 in the center of two vortices. The radial velocity has largest positive amplitude, where Z_3=10.96 is located at the middle position of two-vortex pair.

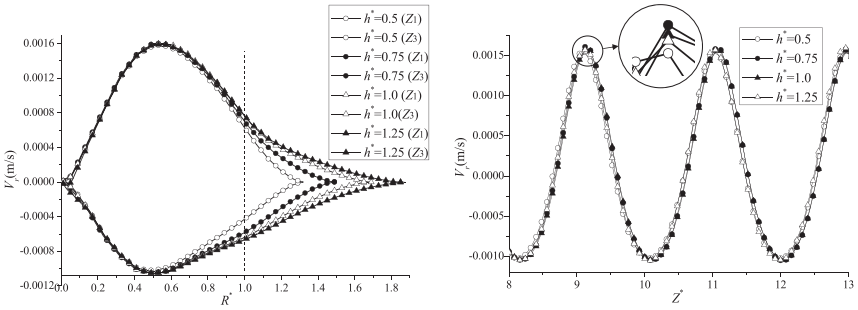

(a) (b)

Figure 6. Radial velocity distribution in different h^* slit models.

(a) At the position of Z_1=10.06 and Z_3=10.96, (b) in the middle position of the annular gap (=0.5).

In order to find the slit aspect ratio effect on the radial flow velocity, the radial velocity at the positions, which have a larger velocity amplitude, is compared in different slit models, which is shown in Figure 6(a). There is a dotted line (R^*=1.0) dividing the flow field in the annular gap from the flow field in the slit wall region. It is clear that the radial velocity of model h^*= 0.5 is the smallest in the annular gap, but the difference of the other three models was not significant. In Figure 6(a), it can be found that the radial velocity amplitude at the R^*=0.5 location is the largest, so the radial velocity of different models in the middle position of the annular gap is extracted in Figure 6(b). The wave period and frequency of the four models are basically the same, and the positive radial velocity amplitude of h^*=0.75 is 4.5% larger than that of model h^*=0.5, 1.3% larger than that of model h^*=1.0, and 2.3% larger than that of model h^*=1.25.

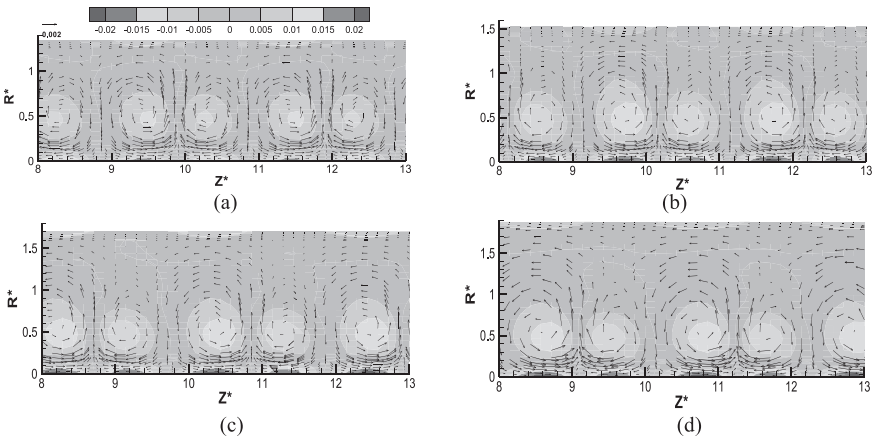

Figure 7. Velocity and vorticity distribution in R-Z plane under non-isothermal conditions.

(a) h^*=0.5, (b) h^*=0.75, (c) h^*=1.0, (d) h^*=1.25 (Re=115).

Figure 7 shows the velocity and vorticity in R-Z plane of different slit models when Re=115. Compared with the result in Figure 4, the axial position of the Taylor vortex has obviously changed, and the variable quantity of the vorticity has also explicitly changed.

Table 1. The Taylor vortex axial dimension of different models.

	h^*=0.5	h^*=0.75	h^*=1.0	h^*=1.25
$\lambda(Re$=115)	1.6d	2.0d	2.04d	2.08d
$\lambda(Re$=132)	1.6d	1.68d	1.71d	1.78d

Table 1 shows the axial dimension of the Taylor vortex (λ) of different models in R-Z plane. It can be found that the axial dimension of the Taylor vortex increases with the slit aspect ratio. When Re is 115, the vortex axial size of h^*=0.75 model is 2.04% higher than that of h^*=0.5 model, the vortex axial size of h^*=1.0 model is 2% higher than that of h^*=0.75 model, and the vortex axial size of h^*=1.25 model is 2% higher than that of h^*=1.0 model. Meanwhile, when Re is equal to 132, the vortex axial size of h^*=1.25 model is also the largest among the four different models. Thus, the slit wall depth, affected by the temperature gradient, has a promoting effect on the Taylor vortex axial size. However, the vortex axial size at Re=132 appears to be smaller than that at Re=115.

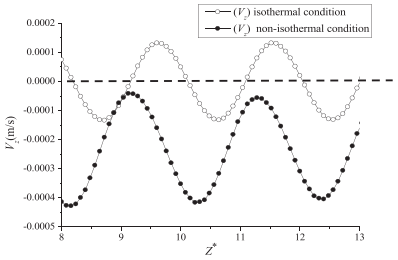

Figure 8. The axial velocity distribution near the outer wall at different conditions.

Figure 8 shows the axial velocity distribution of model h^*=1 at R^*=1.61 near the outer wall under isothermal and non-isothermal conditions. It can be found that, under isothermal conditions, the axial flow direction velocity changes periodically, which is symmetric with respect to a line marked in Figure 8. Under non-isothermal conditions, the axial velocity changes regularly, but the flow direction is always from the top to the bottom. In the present study, the temperature of the outer cylinder is lower than that of the inner cylinder. Therefore, the fluid near the outer cylinder has the tendency of moving towards the bottom direction.

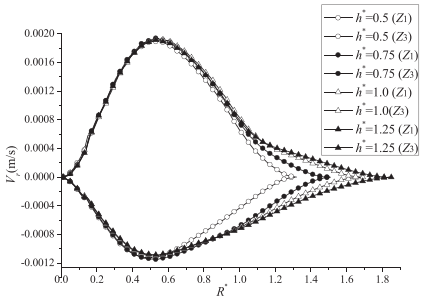

Figure 9. Radial velocity distribution in different slit models at non-isothermal conditions (Re=115).

Figure 9 shows the radial velocity of different slit models at the positions of Z_1, Z_3. It can be found that the positive radial velocity amplitude of h^*=0.75 is 2.6% larger than that of h^*=0.5, and the negative radial velocity amplitude of h^*=0.75 is 5.5% larger than that of h^*=1.0 and h^*=1.25, and this means that the radial velocity of the lower temperature fluid flows from the outer cylinder to the inner one is the largest. Compared with Figure 6(a), the positive radial velocity amplitude of h^*=0.75 is increased by 21.3%. It demonstrates the slit aspect ratio effect on the fluid motion in the annular gap.

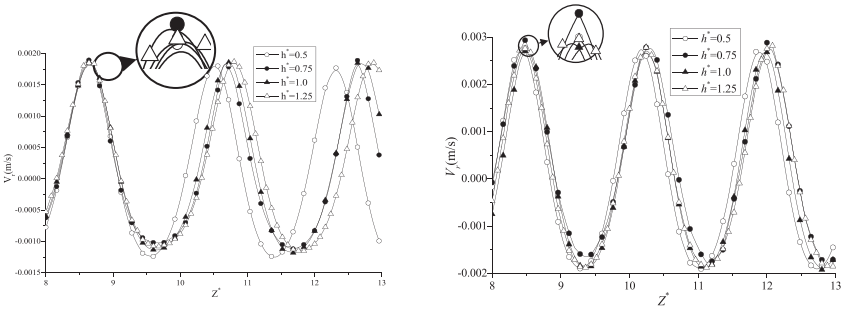

Figure 10. Radial velocity distribution of different slit models at R^*=0.5. (a) Re=115, (b) Re=132.

Figure 10 shows the radial velocity distribution in the middle of the annular gap, while the Reynolds number is 115 and 132. In Figure 10(a), compared with the slit models of h^*=0.5, h^*=1.0, and h^*=1.25, the positive radial velocity amplitude of h^*=0.75 increased by 3.3%, 1.6%, and 1.6%, respectively, and the negative radial velocity amplitude of h^*=0.75 is also the greatest among the four different slit models. In Figure 10(b), the maximum radial velocity in h^*=0.75 model also has the largest value among the four models at Re=132. Compared with the slit model of h^*=0.5, h^*=1.0, and h^*=1.25, the positive radial velocity amplitude of h^*=0.75 increased by 3.9%, 5.4%, and 3.9%, respectively. This conclusion is similar to the condition when Gr=0. It proves that the depth of slit within a certain range can strengthen the radial flow motion in the annular gap, and the radial flow will obviously be weakened as the slit depth increases further.

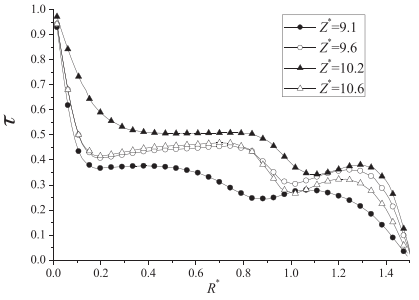

Figure 11. The dimensionless radial temperature distribution along the axial position (h^*=0.75, Re=115).

The dimensionless radial temperature is defined as $\tau = (T-T_{out})/(T_{in}-T_{out})$, and the distribution of τ at different axial positions in model h^*=0.75 is shown in Figure 11. The four different axial positions are shown, which are the area between two-vortex pair, the center of the clockwise

vortices, the position between two vortices in a vortex pair, and the center of the counterclockwise vortices, respectively. It can be found that τ near the inner and outer cylinder walls is larger, and when R^* is within 0.2 to 0.9, the temperature nearly keeps constant except Z^*=9.1. In the area between the two-vortex pair, where Z^*=9.1, the temperature gradient between the fluid and the inner cylinder wall is larger than that in other places. Because of the larger negative radial velocity in this area, the lower temperature fluid flows from the outer cylinder to the inner one. When Z^* is 10.2, the τ between the fluid and the outer cylinder wall is larger than that in other places. This is because the fluid in this area has a larger positive radial velocity, and the higher temperature fluid flows from the inner cylinder to the outer one. In conclusion, the area between the two-vortex pair near the inner wall has a larger temperature gradient, and the temperature profile of different models at the positions is depicted in Figure 12.

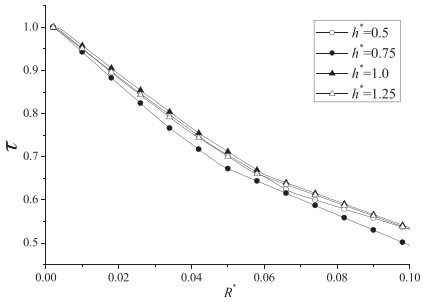

Figure 12. The dimensionless radial temperature distributions near the inner cylinder wall (*Re*=115).

The dimensionless radial temperature distribution in the four different models along the radial direction near the inner surface ranging from R^* = 0 to R^* = 0.1 is shown in Figure 12. The temperature gradient of the fluid to the inner cylinder wall in h^*=0.75 model increased by 4.13%, 4.05%, and 4.06%, compared with the models of h^*=0.5, h^*=1.0, and h^*=1.25.

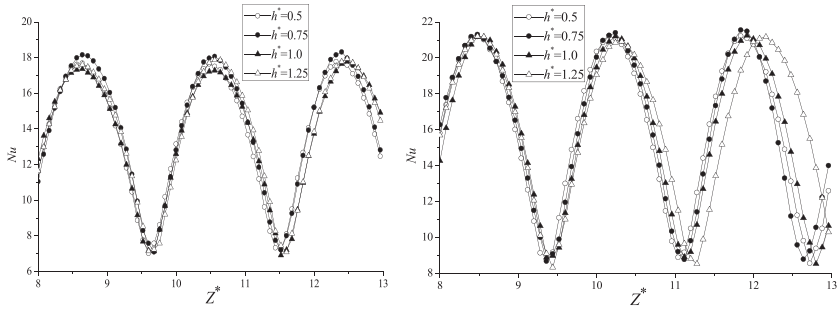

Figure 13. Nusselt number distribution near the inner cylinder of different slit models.

(a) *Re*=115, (b) *Re*=132.

Figure 13 shows the Nusselt number (*Nu*) distribution near the inner cylinder wall ($R^*\approx0$) in different slit models, while the Reynolds number is 115 and 132. It can be seen that the maximum *Nu* number is in h^*=0.75 model and remains to be the largest in the four models at two different

Reynolds numbers. In order to further verify the results, the average Nusselt number near the inner cylinder wall at different Reynolds numbers is shown in Figure 14. It is clear that the average Nusselt number increases when h^* varies from 0 to 0.75 and decreases from 1 to 1.25. When Re =115, the average Nusselt number in h^*=0.75 model is approximately 3% higher than that in the other models. From this figure, it can be found that the average Nusselt number increases with the Reynolds number. Meanwhile, the average Nusselt number of h^*=0.75 model at different Reynolds numbers is always the largest among the four models. In the present study, the temperature of the inner and outer cylinder walls remains constant, and the additional heat is dissipated through the outer cylinder. Therefore, the higher average $\overline{Nu}$ near the inner cylinder wall shows the stronger ability of heat transfer, which means that the h^*=0.75 model has the best heat transfer efficiency.

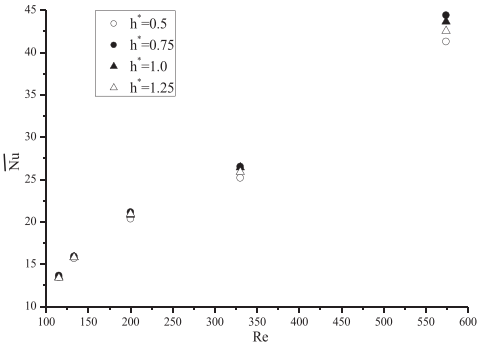

Figure 14. The average Nusselt number of different models at different Reynolds numbers.

CONCLUSION

Taylor-Couette flow in different slit models was studied by numerical simulation. The influence of the slit aspect ratio on the radial flow velocity, with and without temperature gradient, is analyzed. By comparing the Nusselt numbers on the inner cylinder wall, the model with best heat transfer efficiency was found. The main conclusion can be made as follows. The positive and negative radial velocity amplitudes of h^*=0.75 are the largest among the four different models. The temperature gradient of the fluid near the inner cylinder to the wall has the maximum value in the model with an aspect ratio of 0.75. The Nusselt number increases with the Reynolds number, and the average Nusselt number in h^*=0.75 model is the largest among the four models.

ACKNOWLEDGMENT

This study was supported by the National Natural Science Foundation of China (51676086 and 51206062), Natural Science Foundation of Jiangsu Province (BK20161351 and BK20141302), China Postdoctoral Science Foundation (2017M610305), and Six Talent Peaks Project of Jiangsu Province (2014-ZBZZ-016).

REFERENCES

Deters, T. & Egbers, C. 2005. The Taylor-Couette system with radial temperature gradient. Journal of Physics: Conference Series **14**(1): 138-142.

Fénot, M., Dorignac, E., Giret, A. & Lalizel, G. 2013. Convective heat transfer in the entry region of an annular channel with slotted rotating inner cylinder. Applied Thermal Engineering. **54**(1): 345-358.

Jeng, T. M., Tzeng, S. C. & Lin, C. H. 2007. Heat transfer enhancement of Taylor–Couette–Poiseuille flow in an annulus by mounting longitudinal ribs on the rotating inner cylinder. International Journal of Heat and Mass Transfer. **50**(50): 381-390.

Kádár, R. & Balan, C. 2012. Transient dynamics of the wavy regime in Taylor–Couette geometry. European Journal of Mechanics-B/Fluids **31**: 158-167.

Kiełczewski, K., Tuliszka-Sznitko, E. & Bontoux, P. 2014. Numerical investigation of the Taylor-Couette and Batchelor flows with heat transfer: Physics and numerical modeling. Journal of Physics: Conference Series **530**(1): 012037

Lee, S. H., Chung, H. T., Park, C. W. & Kim, H. B. 2009. Experimental investigation of the effect of axial wall slits on Taylor-Couette flow. Fluid Dynamics Research, **41**(4), 730-742.

Lee, Y. N. & Minkowycz, W. J. 1989. Heat transfer characteristics of the annulus of two coaxial cylinders with one cylinder rotating. International journal of heat and mass transfer. **32**(4): 711-722.

Liu, D., Wang, Y. Z., Shi, W. D., Kim, H. B. & Tang, A. K. 2015. Slit wall and heat transfer effect on the Taylor vortex flow. Energies. **8**(3): 1958-1974.

Liu, D., Lee, S. H. & Kim, H. B. 2010. Effect of a constant radial temperature gradient on a Taylor-Couette flow with axial wall slits. Fluid Dynamics Research, **42**(6): 965-974.

Sun, Y. X., Zhao, X. F. & Wu, B. 2012. Numerical simulation of convective heat transfer in annular gap between rotating inner cylinder and concentric fixed outer cylinder. Journal of Wuhan Textile University, **25**(6):81-86

Taylor, G. I. 1923. Stability of a viscous liquid contained between two rotating cylinders. Philosophical Transactions of the Royal Society of London. Series A, Containing Papers of a Mathematical or Physical Character **223**: 289-343.

Tzeng, S. C. 2006. Heat transfer in a small gap between co-axial rotating cylinders. International communications in heat and mass transfer. **33**(6): 737-743.

Zhu, F., Liu, D., Chao, C., Zhang, P. & Yan, J. 2015. Effect of exterior cylinder slit wall on wavy vortex flow in gap of concentric cylinders. Journal of Drainage & Irrigation Machinery Engineering, **33**(6):516 -520.

Submitted: 18/02/2016
Revised : 04/11/2016
Accepted : 18/12/2016